International Journal of Applied Earth Observations and Geoinformation 105 (2021) 102614

Contents lists available at ScienceDirect

International Journal of Applied Earth Observations and Geoinformation

journal homepage: www.elsevier.com/locate/jag

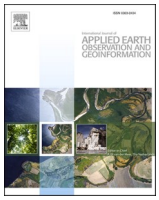

Spatio-temporal prediction of soil moisture and soil strength by depth-to-water maps

Marian Schönauer [a,*], Kari Väätäinen [b], Robert Prinz [b], Harri Lindeman [b], Dariusz Pszenny [c], Martin Jansen [d], Joachim Maack [a], Bruce Talbot [e], Rasmus Astrup [e], Dirk Jaeger [a]

[a] Department of Forest Work Science and Engineering, University of Göttingen, Göttingen, Germany
[b] Natural Resources Institute Finland (Luke), Helsinki, Finland
[c] Warsaw University of Life Sciences – SGGW, Warsaw, Poland
[d] Department of Soil Science of Temperate Ecosystems, University of Göttingen, Göttingen, Germany
[e] Norwegian Institute of Bioeconomy Research (NIBIO), Ås, Norway

ARTICLE INFO

Keywords:
Depth-to-water
Soil moisture content
Precision forestry
Trafficability prediction
Forest operations
Soil bearing capacity

ABSTRACT

The utilization of detailed digital terrain models entails an enhanced basis for supporting sustainable forest management, including the reduction of soil impacts through predictions of site trafficability during mechanized harvesting operations. Since wet soils are prone to traffic-induced damages, soil moisture is incorporated into several systems for spatial predictions of trafficability. Yet, only few systems consider temporal dynamics of soil moisture, impeding the accuracy and practical value of predictions. The depth-to-water (DTW) algorithm calculates a cartographic index which indicates wet areas. Temporal dynamics of soil moisture are simulated by different DTW map-scenarios derived from set flow initiation areas (FIA). However, the concept of simulating seasonal moisture conditions by DTW map-scenarios was not analyzed so far. Therefore, we conducted field campaigns at six study sites across Europe, capturing time-series of soil moisture and soil strength along several transects which crossed predicted wet areas. Assuming overall dry conditions (FIA = 4.00 ha), DTW predicted 20% of measuring points to be wet. When a FIA of 1.00 ha (moist conditions) or 0.25 ha (wet conditions) were applied, DTW predicted 29% or 58% of points to be wet, respectively. De facto, 82% of moisture measurements were predicted correctly by the map-scenario for overall dry conditions – with 44% of wet measurements deviating from predictions made. The prediction of soil strength was less successful, with 66% of low values occurring on areas where DTW indicated dryer soils and subsequently a sufficient trafficability. The condition-specific usage of different map-scenarios did not improve the accuracy of predictions, as compared to static map-scenarios, chosen for each site. We assume that site-specific and non-linear hydrological processes compromise the generalized assumptions of simulating overall moisture conditions by different FIA.

1. Introduction

High resolution digital elevation models (DEM) have become state-of-the-art in supporting sustainable forest management. One of many applications of such models is given through cartographic indices, which are used for predicting trafficability across forest sites. Current site trafficability is an important factor to consider during forest operations with heavy machines. As a result of this, such operations used to be executed during winter, when ground was frozen. Soil impacts are commonly low then, since frozen mineral soils possess a high soil strength (Bates et al., 1993). However, a change of weather regime across large parts of Europe made it difficult to conduct the entirety of annual harvesting operations in periods of favorable conditions. Intensive precipitations during summer and a lack of winter frosts (Climate Service Center Germany) will shorten such periods. Especially when soils plasticity limit is reached during periods of high moisture, traffic can result in severe soil displacement (Horn et al., 2007; Poltorak et al., 2018; Labelle and Jaeger, 2019; Uusitalo et al., 2020), with long-lasting

* Corresponding author at: Department of Forest Work Science and Engineering, University of Göttingen, Büsgenweg 4, Göttingen 37077.
E-mail addresses: marian.schoenauer@uni-goettingen.de (M. Schönauer), kari.vaatainen@luke.fi (K. Väätäinen), robert.prinz@luke.fi (R. Prinz), harri.lindeman@luke.fi (H. Lindeman), dariusz_pszenny@sggw.edu.pl (D. Pszenny), mjansen@gwdg.de (M. Jansen), joachim.maack@uni-goettingen.de (J. Maack), bruce.talbot@nibio.no (B. Talbot), rasmus.astrup@nibio.no (R. Astrup), dirk.jaeger@uni-goettingen.de (D. Jaeger).

https://doi.org/10.1016/j.jag.2021.102614
Received 19 May 2021; Received in revised form 2 November 2021; Accepted 7 November 2021
Available online 16 November 2021

Fig. 1. Locations of the study areas, where time-series of soil strength and moisture measurements were performed and compared to different scenarios of depth-to-water maps.

(Rab, 2004; Sohrabi et al., 2021) consequences towards forest growth and microbiological activity (Beylich et al., 2010).

To enable eco-efficient and therefore sustainable forest management, numerous approaches were established for predicting trafficability, including the creation of maps showing sensitive areas. The high spatial resolution of DEMs available is supposed to embrace highest possible accuracy for such maps (Vega-Nieva et al., 2009; White et al., 2012; Jones and Arp, 2017). However, commoly applied systems provide static information about trafficability but do not consider temporarily changing site conditions. Changing site conditions are driven by temporal and spatial variations of soil moisture, known to have an effect on soil strength and correlate with the extent and degree of soil-impacts like deep ruts (McNabb et al., 2001; Cambi et al., 2015; Poltorak et al., 2018; Uusitalo et al., 2020).

The depth-to-water (DTW) concept was conceived, developed and tested at the University of New Brunswick (Faculty of Forestry and Environmental Management), by Fan-Rui Meng, Jae Ogilvie and Paul Arp, as described by Murphy et al. (2007, 2009, 2011). DTW is based on the utilization of geo-spatial data and is renowned as a robust tool for the prediction of perennial streams, wet or water saturated areas, and sensitive areas for ground-based trafficking (Murphy et al., 2011; Ågren et al., 2014; Ågren et al., 2015; Mohtashami et al., 2017; Väätäinen et al., 2019). When calculating DTW maps, in a first step, local depressions are removed by using a fill-function (e.g. Tarboton, 1997). Afterwards, a flow accumulation tool (D8, O'Callaghan and Mark, 1984) is applied and the resultant accumulation is further used to define starting points. The starting points are set by an adjustable value of the upstream contributing areas' size and used to initiate flow paths. Subsequently, the DEM is used to delineate the shortest vertical difference between each surface grid cell and adjacent flow paths: The vertical difference is minimized by the use of a least-cost function, applied onto least cumulative slopes between each grid cell and adjacent flow paths. The process ensures the assignment of each surface grid cell to the nearest downslope flow path with the most likely hydrological connection. Accordingly, low values of DTW indicate moist or water saturated conditions, while high values indicate well drained areas. This concept is numerically robust and can be applied to DEMs of different spatial resolutions (Ågren et al., 2014). Yet, the resolution of the used input data should not exceed 5–10 m, to guarantee a practical value of the created maps for forest operations.

When applying the DTW algorithm, temporal variations of trafficability are simulated by means of several scenarios of created maps, each representing a different overall moisture regime at the site. This is facilitated by condensing and extending upstream contribution areas (FIA) for initiating flow lines across the landscape. Subsequently, small FIAs represent a high soil moisture at a site, whereas a large FIA would represent dryer conditions. The map scenarios cover conditions reaching from "very dry or frozen" to "wet" (Jones and Arp, 2019). Accordingly, the user of such DTW maps can individually choose the most reliable scenario for a given time and site of harvesting operation.

In large Canadian forestry companies, high-resolution accessibility maps based on wet-areas mapping (Murphy et al., 2009) are being used in combination with DTW to minimize traffic damage to forest soil through improved resource road planning (Vega-Nieva et al., 2009;

Table 1
Characteristics of the study sites, where a validation of depth-to-water maps was conducted.

	Site	Country		
		[1]Finland	[2]Germany	[3]Poland
Region		North-Karelia	Sauerland, North-Rhine-Westphalia	South Poland, Border of Silesian and Lodz Voivodeship
Coordinates (long/lat)	A	29.625486	8.017874	19.492248
	A	62.653529	51.477830	50.954030
EPSG: 4326	B	30.16780	8.038702	19.535888
	B	62.775407	51.406658	50.903021
Elevation [m]	A	110	270	217
	B	110	260	220
Geology		Migmatitic tonalite, biotite paragneiss and granite	Claystone and Sandstone from Devon and Karbon	Sands and gravels and tills as well as glacial sands and gravels
Soil types		Haplic Podzol, Histosol	Cambisol, Stagnosol	Haplic Podzol
Texture class		loamy sand	silty loam	sand
Soil bulk density [g cm^{-3}]		1.20	1.20	1.60
[4]**Humus form**	A	Dysmoder	Mull	Dysmoder
	B	Humimor	Mesomull	Dysmoder
Mean Temp.		[5]2.5 °C	[6]8.9 °C	[7]7.9 °C
Mean annual precipitation		[5]600 mm	[6]790 mm	[7]580 mm
Tree species		*Pinus sylvestris, Picea abies, Betula pubescens*	*Fagus sylvatica, Picea abies, Pinus sylvestris*	*Pinus sylvestris, Larix decidua, Picea abies*

[1] Site A: Onttola, Site B: Eno
[2] Site A: Neheim, Site B: Obereimer
[3] Site A: North, Site B: South
[4] According to Zanella et al. (2011).
[5] Finnish Meteorological Institute (2021).
[6] Deutscher Wetterdienst (2019).
[7] IMGW-PIB (2021).

Campbell et al., 2013). In addition, DTW maps were recently related with species abundance and used for ecological monitoring (Oltean et al., 2016; Bartels et al., 2018). In Sweden, DTW-maps or DTW-like systems have been utilized for roughly six years in planning of loggings and during logging operations (Ågren et al., 2014; Väätäinen et al., 2019). In Finland, soil moisture was derived from digital terrain models and the risk of damage from traffic on rural roads was estimated (Niemi et al., 2017). Recent research reveals potential improvements of such topographic soil wetness indices through a merge with open spatial data and different machine learning approaches (Lidberg et al., 2020; Salmivaara et al., 2020; Schönauer et al., 2021).

Although DTW maps and possible applications have been evaluated extensively, we identified two research gaps: (I.) While numerous implementations of the DTW algorithm were performed and studied in boreal forests of Scandinavia and Northern America, such measures are lacking in temperate forests, for large areas of Europe. (II.) The scenarios of DTW maps, as made through specific settings of the FIA, are envisaged to represent seasonal variations of moisture and therefore soil strength in forest stands. Prior research conjectured the ability to capture such varying conditions by these scenarios, but the concept lacks strong empirical evidence. Consequently, we formulated two research questions:

Can differences in the quality of DTW-predictions of soil moisture and strength be observed between the study sites and attributed to site characteristics?
Can spatio-temporal variations of soil moisture and strength be predicted by the DTW map-scenarios?

To answer these questions, different DTW scenarios were compared to time-series of in-situ measurements, conducted on six study sites in three European countries. We captured temporal and spatial variations of soil moisture content and soil strength by repeated measurements across 24 transects.

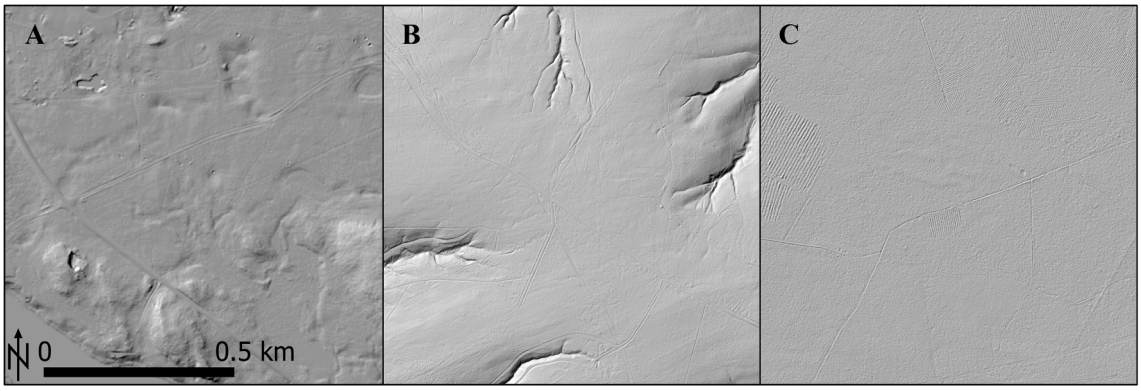

Fig. 2. The topography-based depth-to-water index was calculated based on digital elevation models (hill-shaded), derived from airborne laserscannings, on sites in Finland (A), Germany (B) and Poland (C).

Table 2
Data sources of digital elevation models used to calculate depth-to-water maps.

Country	Data provider	Cell size [m]	Point density [points m^{-2}]	Accuracy [m]	Year of flight
Finland	National Land Survey of Finland	2.0	≥0.5	±0.3	2019
Germany	Bezirksregierung Köln	1.0	4–10	±0.2	2019
[1]Poland	Polish Main Office of Geodesy and Cartography	1.0	4–12	±0.10 to ±0.15	2020

[1] Kurczyński and Bakuła (2013).

2. Material and methods

2.1. Study sites

Field measurements were conducted in three countries: Finland, Germany and Poland (Fig. 1, Table 1). In each of the three countries, two study sites were established in mature forest stands, under closed, homogeneous canopy. Together with local experts, approximately 1,000 ha large study sites, known to be temporarily inaccessible because of low soil strength, were selected on flat or moderately sloped terrain (<35%).

2.2. Depth-to-water maps

A DEM with a sufficiently high spatial resolution is the only necessary input data to calculate DTW maps. Within this study, DEMs derived from airborne laserscanning campaigns (Fig. 2), provided by respective governmental authorities (Table 2), were used to create DTW maps covering the selected sites.

The maps generated for each flow initiation area (FIA) are given as grids of the metric DTW index (e.g. $DTW_{0.25}$ for FIA = 0.25 ha, [m]), with a grid size equal to the input layer. To create DTW maps, the already described procedure, e.g., Murphy et al. (2009, 2011), was recreated in the programming environment R (R Core Team, 2020), using the package "rgrass7" (Bivand, 2021), which provides an interface to run commands from the free toolbox GRASS GIS (Awaida and Westervelt, 2020) in R. To spread the DTW concept, the commented R-script was made openly available: (Schönauer and Maack, 2021), doi:10.5281/zenodo.5638517.

For the present study, three scenarios of DTW maps were created, using FIAs according to Jones and Arp (2019), who stated likely FIAs for different seasons and moisture conditions. This were 4.00 ha, 1.00 ha and 0.25 ha, simulating generally *dry*, *moist* or *wet* soil conditions, respectively (Fig. 3).

2.3. Field measurements

2.3.1. Transects

Each study site contained four transects. Three of these transects were centered perpendicularly across mapped sensitive areas, according to the DTW maps. The transect "4.00" crossed a delineated wet area ($DTW_{4.0}$ < 1 m), calculated using a FIA of 4.00 ha (Fig. 3 A). Accordingly, transects "1.00" and "0.25" crossed wet areas, generated when the algorithm was run with 1.00 ha or 0.25 ha FIA, respectively (Fig. 3 B, C). The fourth transect was located apart from mapped sensitive areas, to serve as control ("exp", Fig. 3). Each transect had a length of 40 m (resulting in 21 transect points, Fig. 3 c) and was permanently marked with wooden pegs, at its starting and end points. The position of starting and end points were captured by means of a handheld GNSS-device with post-correction of position data, for later analyses within a geographic information system.

2.3.2. Measuring campaigns

In each of the three participating countries, repeated field measuring campaings were conducted once a month. To reveal seasonal and spatial variations, eleven campaigns were captured in Germany, ten campaigns in Poland, and six campaigns were captured in Finland, between September 2019 and November 2020. At the in total 27 measuring campaigns, soil strength and moisture were measured at all transect points. Period-to-period measurements were shifted with an interval of 0.2 m along the transect, to probe undisturbed soil.

2.3.3. Soil penetration resistance

After the removal of coarse litter at the points along the transect (Fig. 3c), penetration resistance was measured threefold at each point at randomly selected spots within the area of 0.2 m × 0.2 m, using a handheld Penetrologger (1.0 cm^2, 60° cone, Eijkelkamp, Netherlands). This device captures the soil penetration resistance [MPa] for each centimeter of penetrated depth by means of a load cell. Values measured between a depth of 10 and 20 cm (Schönauer et al., 2021a) of mineral soil, were averaged for each of the three pseudo replications. Subsequently, these three mean values were averaged giving the cone index (CI).

2.3.4. Soil moisture content

At the same time and position of CI-measurements, volumetric soil moisture content (SMC, [%vol]) was quantified in the topsoil below the

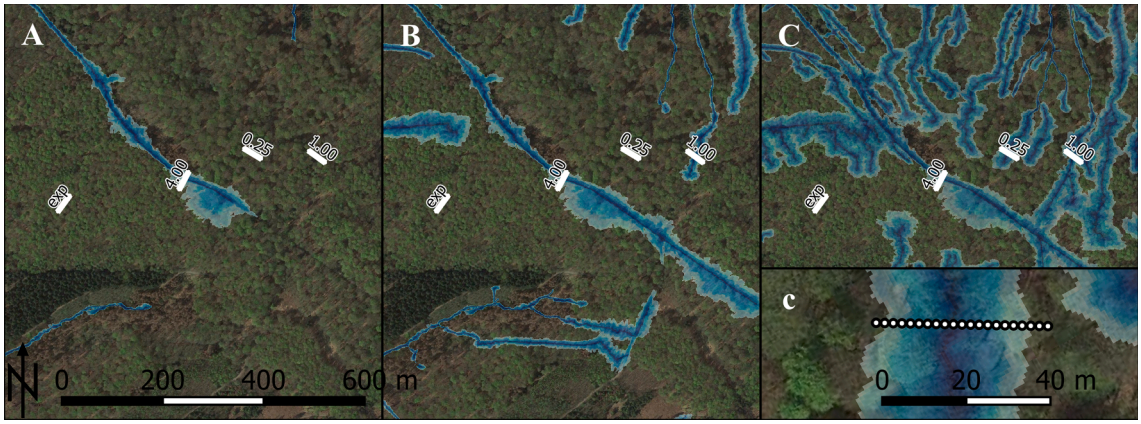

Fig. 3. Three scenarios of depth-to-water (DTW) maps, according to different flow initiation areas (FIA) of 4.00 ha (A), 1.00 ha (B) and 0.25 ha (C). The FIA is defined as required contributing upstream area to start a flow line, with subsequently low values of DTW-index in vertical proximity of those lines (colored blue areas). The Figure shows site A in Germany (Table 1). (For interpretation of the references to colour in this figure legend, the reader is referred to the web version of this article.)

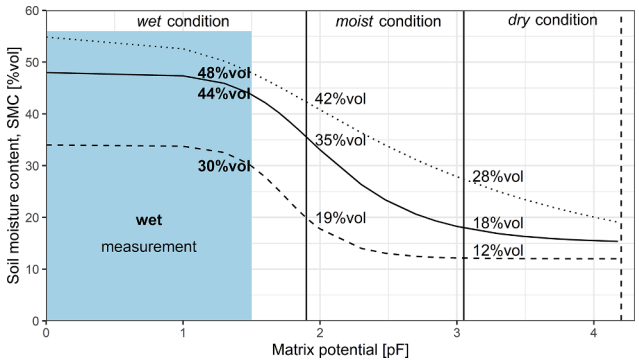

Fig. 4. Texture-specific water retention curves for the study sites in Germany (pointed), Finland (solid) and Poland (dashed). Thresholds (vertical lines, labelled) were applied to mean values of soil moisture content (SMC), grouped by site and campaign. Mean values of SMC above field capacity (1.9 pF) were used to identify *wet* conditions. Centered between field capacity and the permanent wilting point (4.2 pF), the threshold distinguishing between *moist* and *dry* conditions was set (3.05 pF). Each field-measured value was assessed as **wet**, when SMC indicated a low matrix potential (<1.5 pF), as shown by the shading (applied thresholds are given in bold).

litter layer with a impedance measuring technique (HH2-moisture meter, Delta-T-Devices, England). The 57 mm long probes were inserted into the soil from above to measure SMC, which is estimated by the ratio between the volume of water and the total volume of the soil sample (Eijkelkamp, 2013).

2.3.5. Moisture conditions and assigned DTW indices

The conducted measurement campaigns were asserted to three condition classes (*wet*, *moist* and *dry*), with respect to mean values of SMC, grouped by site and campaign. Thresholds between classes of condition were deduced from texture-specific water retention curves (model: 'van Genuchten', Seki, 2007) and are shown in Fig. 4. Therefore, soil probes were taken along the transects and the prevailing texture was estimated according to DIN 19682–2:2007–11. In addition, each measurement of SMC was transformed into binary values, with **wet** values when soils were close to water saturation (<1.5 pF, Fig. 4), and **not-wet** values when the matrix potential was higher than 1.5 pF. In order to give clarity about the used terms, we write '*wet*' when referring to the class of condition, and '**wet**' (binary) when measured SMC on a given transect point and campaign indicated water saturation.

In-field values measured during *dry* conditions were related to $DTW_{4.00}$ maps. When measurements were conducted under *moist* conditions, the resulting values were compared to $DTW_{1.00}$ maps, and values measured during *wet* conditions with $DTW_{0.25}$ maps. Subsequently, the respective index for each moisture condition, was saved as a new variable, DTW_{FIA} (Fig. 5).

2.4. Data analysis

The transects' end- and starting GNSS-positions were transferred to a geographical information system, QGIS, version 3.10.7-A Coruña (QGIS.

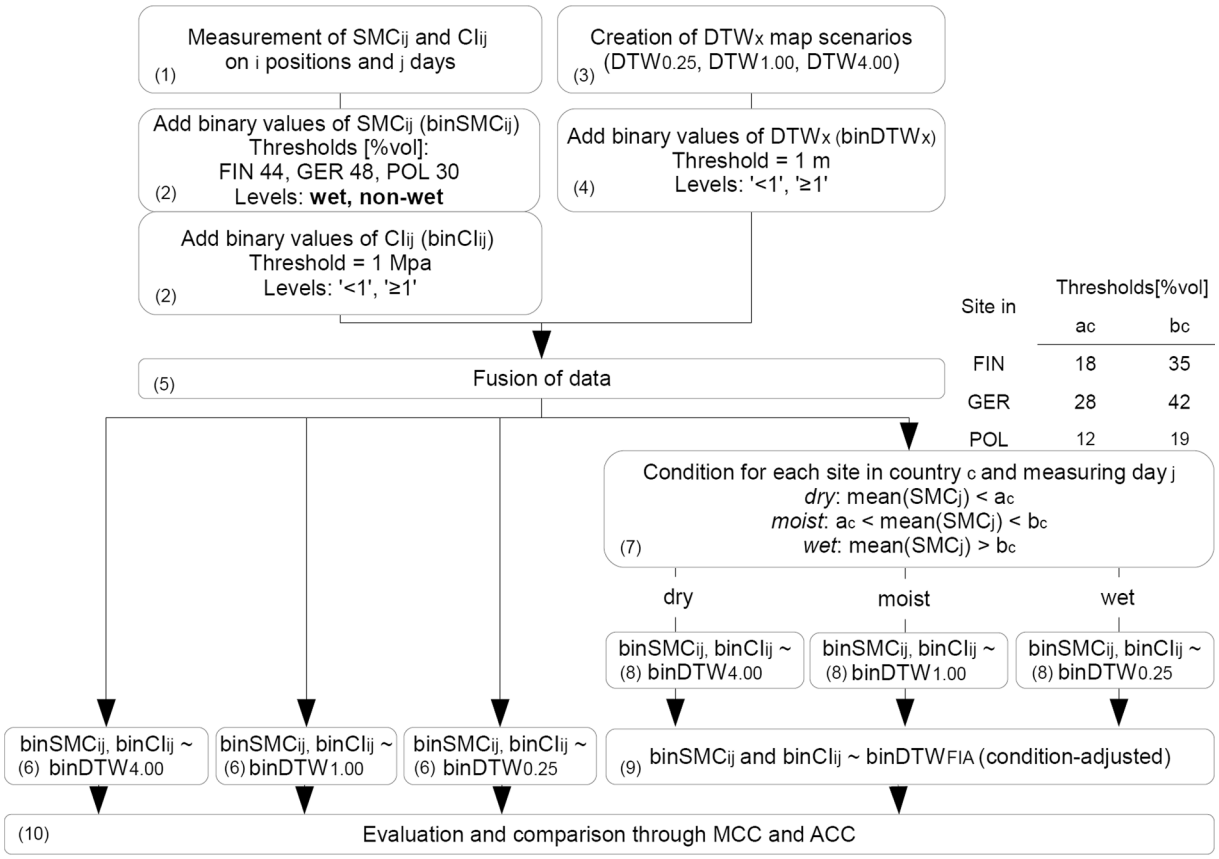

Fig. 5. For assessing the preformance of predictions, the following process was pursued: (1) In-field measurements of soil moisture content (SMCij) and soil strength (CIij) were conducted on i positions (along several transects on sites in FINland, GERmany and POLand) during a time-series of j measuring days. (2) Values of SMCij and CIij were transformed into binaries (binSMCij and binCIij, respectively). (3) Depth-to-water (DTWx) maps were created with different flow initiation areas (x = 0.25 ha, 1.00 ha and 4.00 ha), and (4) transformed into binary values (binDTWx). (5) The data was fused and used for further validations: (6) all values of binSMCij and binCIij were compared to binDTWx; in addition, (7) the data was split by moisture conditions – for that mean values of SMCj of each site and day j were compared with texture-specific moisture thresholds (Fig. 4). This allowed for (8, 9) a condition-adjusted comparison between binSMCij or binCIij and $binDTW_{FIA}$. Finally, (10) a confusion matrix was created and ACC (Eq. (1)) and MCC (Eq. (2)) were calculated.

Table 3
Used confusion matrix to summarize depth-to-water predictions of soil moisture content (binary values of SMC, Fig. 4 and Fig. 5) and binary values of soil strength (CI, Fig. 5). Classes in the matrix, true positives (TP), false positives (FP), true negatives (TN) and false negatives (FN) (Kuhn, 2020) were used for the Eqs. (1) and (2).

	binary SMC		binary CI	
DTW	**wet**	**not-wet**	<1 MPa	≥1 MPa
<1 m	TP	FP	TP	FP
≥ 1 m	FN	TN	FN	TN

org, 2020). The points along the transects were added, considering the spacing of 2 m between points. Since DTW maps are given as raster grids, cell values could be extracted at the measuring points along the transects. The resultant table of attributes, containing the point ID and associated DTW-indices, was exported and merged with data from field measurements and subsequently used for further analyses (Fig. 5). Calculations were performed with the free programming language R (version 4.0.2, R Core Team, 2020), interfaced with RStudio (version 1.4.1103, RStudio, PBC, Boston, MA). Normal distribution of CI and SMC was assessed and approved via QQ-plots. A linear model was used to correlate CI and SMC, with contrasts set to sums for the factors 'country' and 'condition', followed by a type-III ANOVA (Fox and Weisberg, 2019). In addition, a full-factorial linear model was fit to SMC values, followed by a Tukey post-hoc test (Lenth et al., 2019) to compare means between levels of DTW.

2.4.1. Confusion matrix and performance of predictions

The prediction of low soil strength and **wet** soils by means of each DTW index, and by means of a season-adjusted DTW index was assessed, as illustrated in Fig. 5.

The performance of made predictions was assessed via a confusion matrix, with the classes defined in Table 3.

This classification was used to calculate accuracy of prediction (ACC, [%]) and Matthews (1975) correlation coefficient (MCC), according to Eqs. (1) and (2), respectively:

$$ACC = \frac{TP + TN}{TP + TN + FP + FN} \quad (1)$$

$$MCC = \frac{TP*TN - FP*FN}{\sqrt{(TP + FP)(TP + FN)(TN + FP)(TN + FN)}} \quad (2)$$

Linear models using permutation tests (Wheeler et al., 2016) were used to compare ACC and MCC between the usage of static FIAs and those, where FIA was adjusted to the current condition.

Significance level used for all tests was $\alpha = 0.05$. Mean values are given as least squares mean ± standard error.

3. Results

3.1. Soil moisture and strength

Overall soil moisture content (SMC) varied moderately among participating countries between 14.4 ± 0.61 %vol, measured at Polish, and 31.8 ± 0.31 %vol at German study sites (Fig. 6A). The differences of SMC between measuring campaigns were considerable in Germany and Poland. Less variation was observed in Finland, where average values of SMC were between 21.9 ± 1.12 %vol ("Onttola") and 38.40 ± 1.12 %vol ("Eno") only. The entirety of 2,954 observations, measured on 384 points in total, was assigned to the three defined classes of condition, grouped by site and campaign. This resulted in 614 (*dry*), 1840 (*moist*), or 500 (*wet*) values being related to $DTW_{4.00}$, $DTW_{1.00}$ or $DTW_{0.25}$ respectively (Fig. 6).

The occurrence of **wet** values (close to water saturation), related to the entirety of cases, peaked with 35.7% under *wet* conditions on Finnish

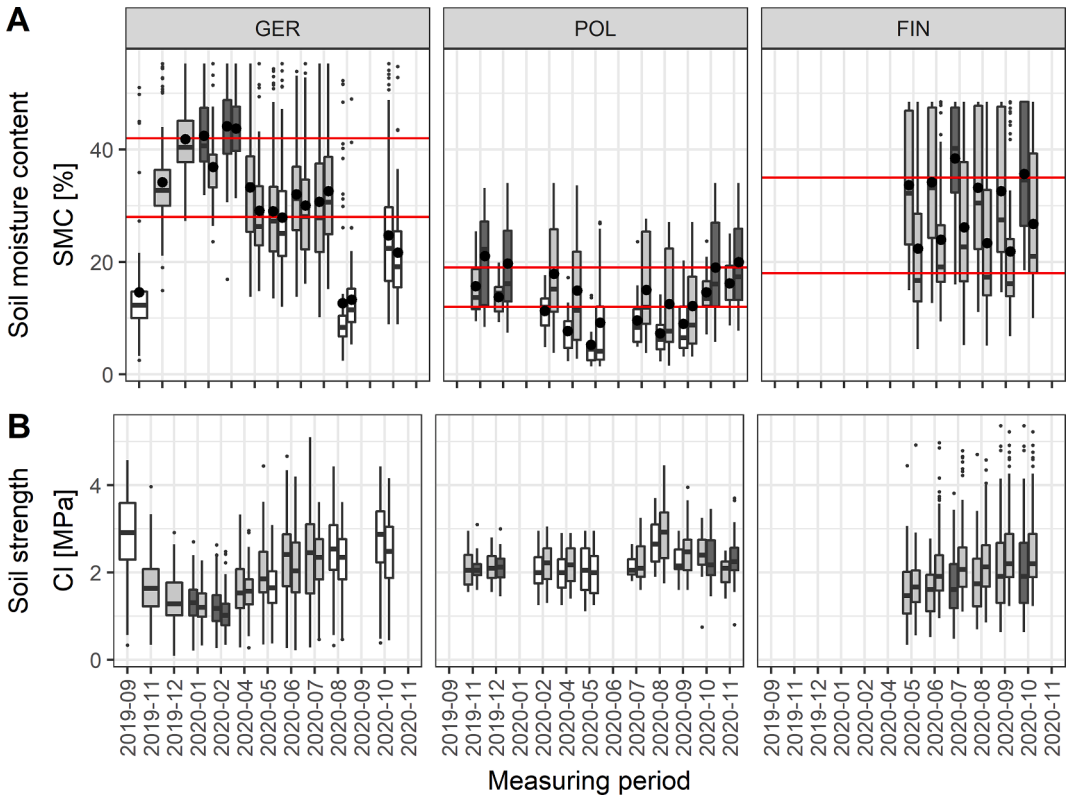

Fig. 6. Monthly repeated measurements of (A) volumetric soil moisture content and (B) soil strength in three countries, grouped by the study site. Defined thresholds (horizontal lines) were applied on mean values of soil moisture (large points) to assign each group to overall moisture conditions (i.e., *dry* - white, *moist* - light gray and *wet* - dark grey, Fig. 4).

Table 4
Type-III ANOVA for the linear model, fitted to values of soil strength (MPa).

	Sum of Squares	Df	F value	Pr(>F)
(Intercept)	1349	1	2257	0
SMC	91	1	152	<0.001
country	96	2	80	<0.001
condition	1.9	2	1.5	0.213
SMC:country	136	2	114	<0.001
SMC:condition	5.4	2	4.5	0.011
Residuals	1726	2887	–	–

Table 5
The table shows an overview of the average terrain slope, the partial area with a depth-to-water index between 0 m and 1 m (calculated with different flow initiation areas) compared to total area of the study sites. In each country, two sites, each 1000 ha in size, were analyzed.

Country	Terrain slope [%]	partial area with DTW<1 m [%]		
		$DTW_{4.00}$	$DTW_{1.00}$	$DTW_{0.25}$
FIN	4.7 ± 6.5	40.4	58.9	77.6
GER	15.5 ± 15.1	10.7	19.9	37.9
POL	1.8 ± 1.9	35.9	62.3	88.8

sites. The low of **wet** measurements was observed on Polish study sites, under *dry* conditions (Fig. 6).

Soil strength, quantified by CI, averaged at 1.82 ± 0.02 MPa on German study sites, and 2.02 ± 0.03 MPa on Finnish ones. In Poland, higher values of CI were measured, averaging at 2.24 ± 0.05 MPa (Fig. 6B). A threshold of 1 MPa was set for CI, with values below this threshold assumed to represent highly traffic-sensitive soils. The proportion of such occurrences did not differ from the frequency of **wet** measurements ($p = 0.212$, unequal variance *t*-test).

Including all data, a response between CI and SMC could be observed ($p < 0.001$), with significant interactions between SMC and country as well as condition, indicating site- and season-specific patterns (Table 4).

3.2. Depth-to-water and soil moisture

Overall, the algorithm detected 47% of the covered area across all study sites as sensitive for soil disturbances, classified when $DTW_{1.00}$ was<1 m (Table 5).

These areas, predicted to be wet or water saturated, were derived from a stream network, with low DTW values nearby. When overall moisture condition was classified as *wet*, all three transects crossed areas with DTW < 1 m (Fig. 3). Under *dry* conditions, only the transect "4.00" crossed an area predicted to be **wet**. This resulted in the behavior shown in Fig. 7.

Subsequently, **wet** values should predominantly occur in areas with $DTW_{FIA} < 1$ m. In fact, up to 100% of **wet** values were measured within a DTW range between 0 and 1 m on the Polish study sites, under given *moist* or *wet* conditions (Fig. 8). Similar to the results revealed in Poland, high shares of **wet** values could be associated with low DTW indices in Finland, too. There, 88% of **wet** values were measured at $DTW_{1.00} < 1$ m or $DTW_{0.25} < 1$ m, when soils were *moist* or *wet*, respectively (Fig. 7 and Fig. 8).

3.3. Prediction of soil moisture and strength

The fact that the extent of areas with DTW < 1 m increases with decreasing FIA or rather *wet* (or *moist*) conditions (Table 5) is particularly considered when Matthews correlation coefficient (MCC) is used to assess the performance of DTW. Overall, ACC for SMC-predictions via DTW_{FIA} averaged at 72%, with corresponding mean MCC of 0.31. When in-situ measurements are related to DTW maps, calculated with FIA set fixed, different assessments of performance were made (Fig. 9), with averages of ACC for each DTW scenario between 51% and 82% and MCC between 0.25 and 0.38. For example, when SMC was predicted by $DTW_{4.00}$ maps, best performance was reached on the study sites "Obereimer" in Germany and "South" in Poland, regardless of the prevalent moisture condition. On the Finnish study site "Eno", FIA of 1.00 ha led to successful prediction of SMC, with MCC of 0.58 and corresponding ACC of 80% under *wet* conditions. During *moist*

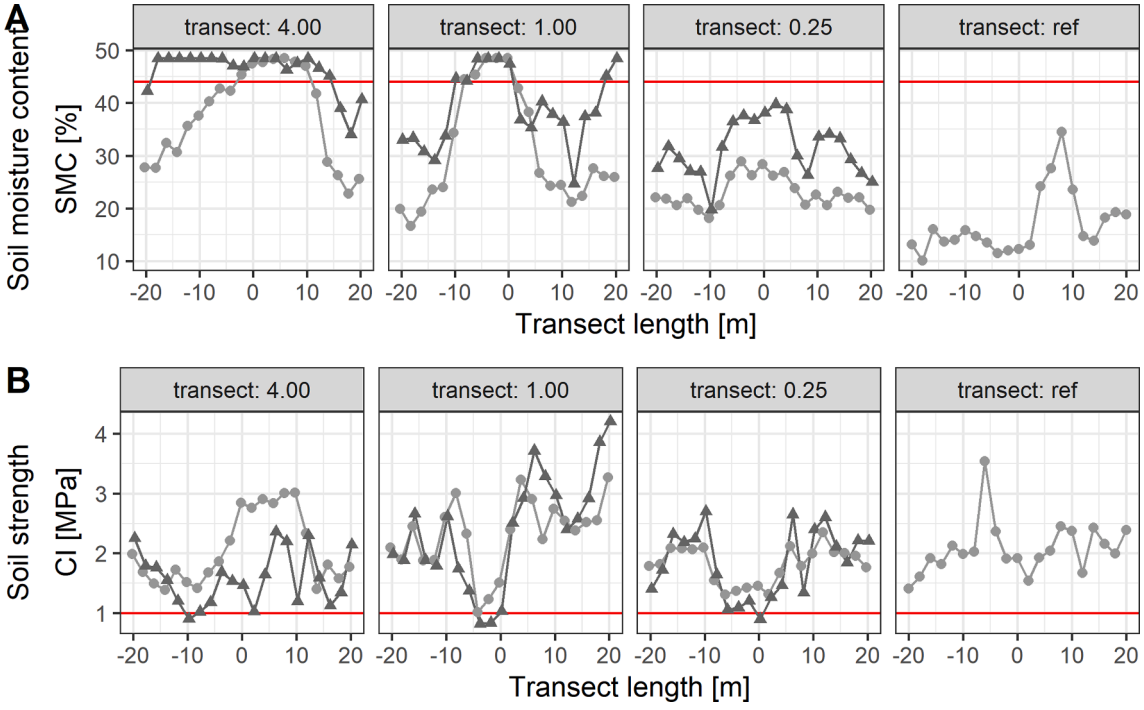

Fig. 7. Values of (A) soil moisture and (B) soil strength along transects, perpendicularly positioned on flow lines (transect length = 0) derived from the depth-to-water algorithm. The examples show data from Finnish study sites, where **wet** soil with low soil strength occurred in proximity to the flow line, during *moist* (filled circle) and *wet* (triangle) conditions on the transect "1.00". Horizontal lines indicate set thresholds to assess **wet** (Fig. 4) or sensitive soils.

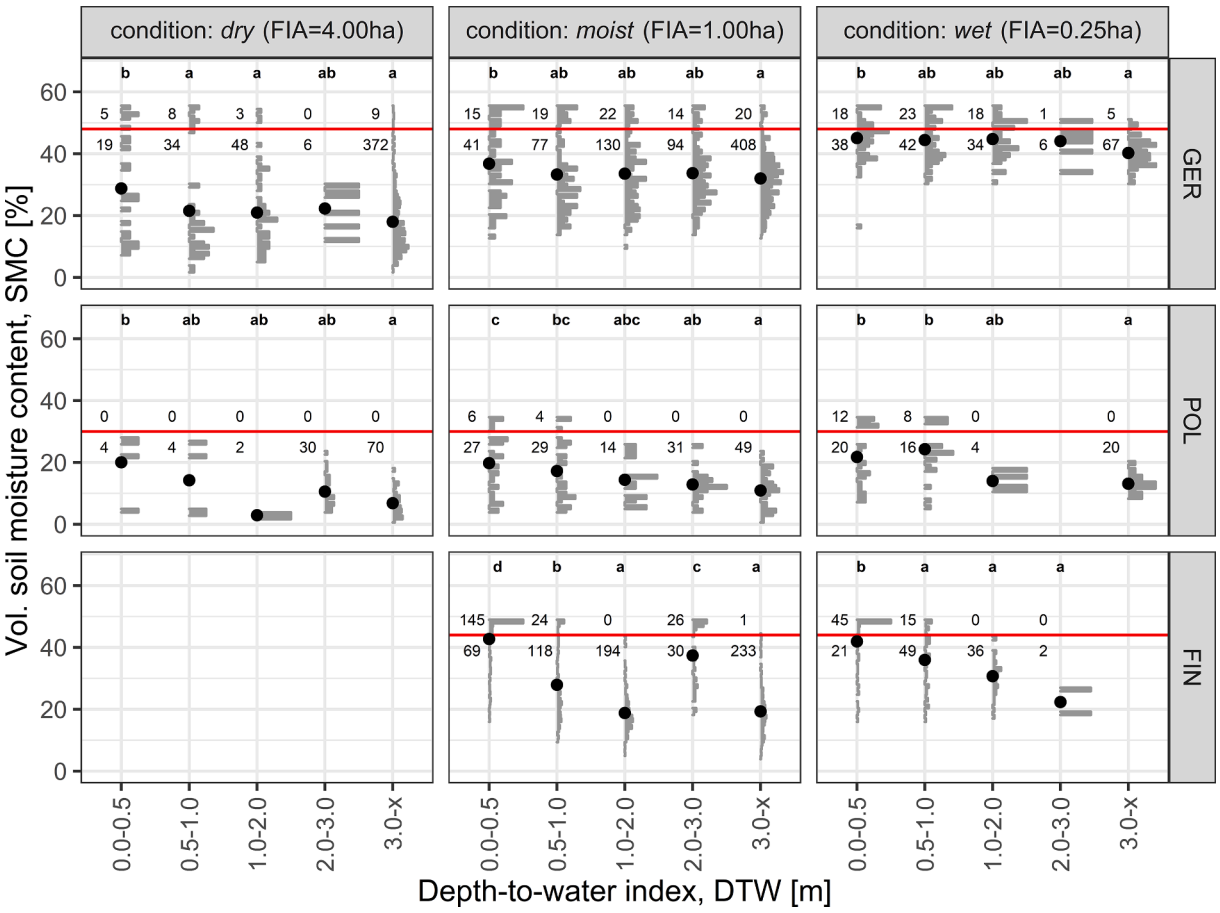

Fig. 8. Values of soil moisture content (SMC) in respect to related depth-to-water (DTW) maps, calculated with different flow initiation areas (FIA), to emulate classes of overall soil moisture condition (Fig. 4). Density of SMC for levels of DTW is shown by histograms. From that, number of SMC-measurements indicating water saturation (Fig. 4) are labeled above the horizontal line. The number of remaining values is given below this line. Mean values are given by points - significant differences between group means are shown by letters according to a Tukey post-hoc test.

conditions on the same site, highest values of performance were retrieved when SMC was compared to $DTW_{1.00}$ too, with 0.51 MCC and 77% ACC.

Improvement of MCC or ACC due to the condition-specific adjustment of FIA could not be observed (Fig. 9), neither for predictions of SMC ($p = 0.327$, $p = 1$, respectively) nor CI ($p = 0.603$ and $p = 1$, respectively).

4. Discussion

The generally close agreement between the occurrence of **wet** soils within areas of a low DTW index (Fig. 8) confirms the main assumption of the algorithm, stating that water moves gravimetrically, following the flow directions as determined by topographic geometry. The consequent accumulation of water across a landscape leads to areas with a high probability for water saturation. In line with this assumption, peaks of MCC for predictions of **wet** soils were between 0.71 and 0.58, with corresponding ACC between 85% and 75%, respectively (Fig. 9). DTW can be assumed to clearly predict soil wetness (Ågren et al., 2014). Across the studied countries, ACC averaged at 82% (MCC = 0.38), when dummy-transformed SMC values were compared to the binary values of $DTW_{4.00}$. These results are in line with earlier findings: Ågren et al. (2014) revealed an accuracy between 72% and 92% with varying FIA between 0.5 ha and 16 ha. In another Swedish case study, Lidberg et al. (2020) revealed an accuracy of 73%. In agreement, the position of existing wet areas has already been delineated by DTW-maps successfully (Murphy et al., 2011). Remote analysis of Murphy et al. (2007) showed, that discrete wetland areas on Canadian study sites were properly reflected by DTW maps in 51%-67% of cases, improving the knowledge of spatial distributions of such at given forest sites.

However, DTW-related predictions of wet soils are not necessarily successful, as reported by Schönauer et al. (2021a), where SMC was measured on random positions across two forest sites, but could not be related to DTW indices significantly. In addition, the same authors (2020) showed that soil strength (CI) did not respond to values of DTW. Also, findings from the Krycklan catchment make a response between CI and DTW look questionable (Ågren et al., 2015).

Site-effects showed high influence on the accuracy of DTW-derived predictions of rut formations (Mohtashami et al., 2017). Characteristics of soil and bedrock can compromise water accumulation, which is the primary factor simulated by DTW maps. Consequently, the shallow Podzol and Histosol on the Finnish study sites should lead to accurate predictions of **wet** soils since a high share of lateral water movement would occur in the upmost layers there (Bishop et al., 2011). Accordingly, the Finnish data demonstrated relatively successful predictions of binary values of SMC by DTW maps, with ACC between 81% and 71% ($DTW_{1.00}$) and corresponding MCC of 0.23 and 0.35, respectively. With respect to effective water runoff predictions in uppermost soil compartments, the well-drained sandy soils on Polish sites should possess least overlap between **wet** soils and DTW < 1 m, as water would drain quickly into deeper horizons there (Singh et al., 2020). However, performance values for the prediction of dummy-transformed SMC were similar as compared to observations made on Finnish data. Although ACC in a comparable range was determined on German sites (47% –

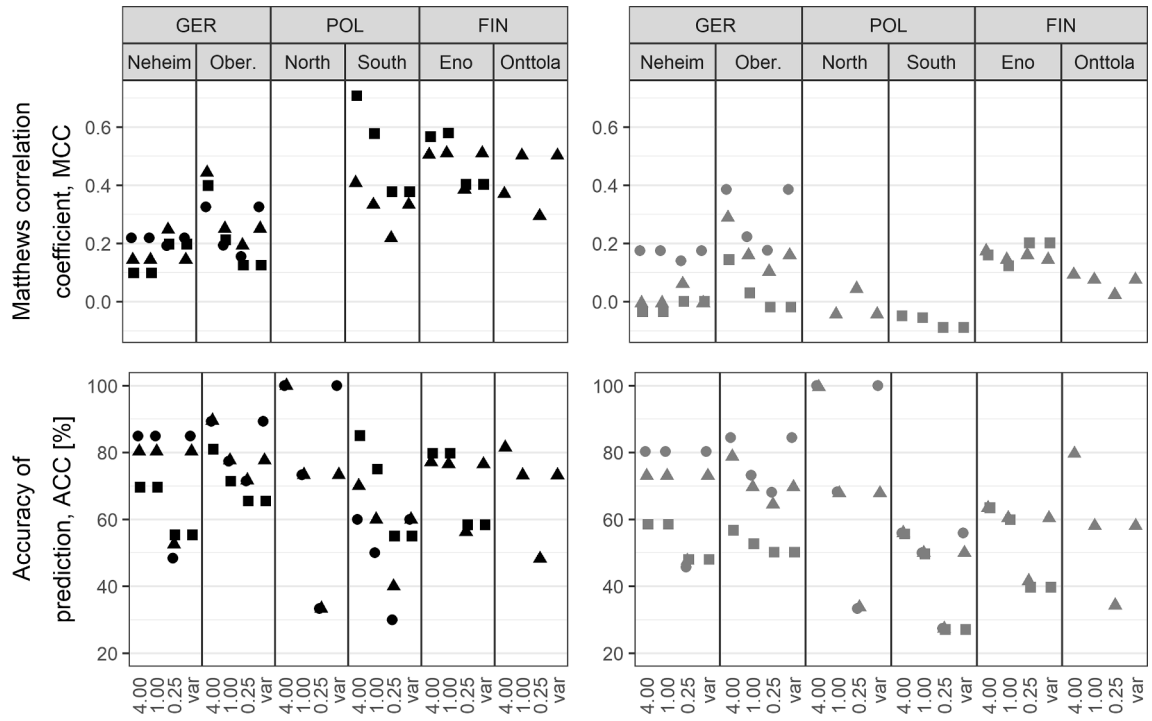

Fig. 9. Accuracy of prediction, when in-situ measurements were related to scenarios of depth-to-water maps, created with static flow initiation areas (FIA) (x-labels), or when FIA was variable according to current conditions ('var', Fig. 4). Black symbols represent binary values of soil moisture content [%], grey symbols represent binary values of soil strength [MPa] (conditions: *wet* – square, *moist* – triangle, *dry* – point).

89%, $DTW_{1.00}$), MCC, the more meaningful parameter for predictions (Powers, 2011), was low (average: 0.18 ± 0.11, Fig. 9). Deep Cambisols with higher water storage capacity could lead to a less linear flow accumulation of precipitation across the landscape. Lower permeability due to the high clay content on German sites should promote the usage of a small FIA. Nevertheless, our findings did not support this assumption in the conducted field trials. On the Cambisols with high clay-content, the largest FIA surveyed (4.00 ha) showed to lead to highest MCC and ACC, at least at the steep site "Obereimer". In contrast, at the second German site "Neheim", a small FIA of 0.25 ha led to best performance.

Instead of representing site-conditions, the FIA-derived scenarios of DTW maps were designed to represent changing overall moisture conditions (White et al., 2012). Yet, we were not able to confirm this idea with the given data. As can be seen in Fig. 9, the season-adjusted DTW did neither improve ACC nor MCC. Most likely, the non-linear behavior of water runoff, in regard to spatial shifts, hydraulic conductivity with soil depth and water storage (Leach et al., 2017) inhibited the intended season- or condition-adjusted prediction of **wet** soils and low CI through DTW maps. The spatial variability in subsurface permeability and hydrological conditions may work against the seasonal simulation of water runoff and accumulation across sites (Ågren et al., 2015; Leach et al., 2017). The real accumulation of water runoff oscillates in accordance with climate, site characteristics and soil properties, making it hard to find a site- and season specific FIA (White et al., 2012; Ågren et al., 2014; Ågren et al., 2015; Leach et al., 2017; Lidberg et al., 2020).

In addition to the disregard of soil-related hydrological conditions, also crucial factors like root network, available slash, stoniness, stumps and at the end soil strength are not considered in DTW maps but are vital for soil trafficability (Suvinen et al., 2009; Vega-Nieva et al., 2009; Ågren et al., 2014; Ågren et al., 2015). Remote sensing techniques offer a way to estimate information about soil properties (Coleman et al., 1993; Dobos et al., 2001) and moisture (Hu et al., 1997). Additionally, vegetation analysis (Ustin and Gamon, 2010; Fassnacht et al., 2016) can be performed using air- or space-borne approaches. These data might allow for an evidence-based estimation of a more accurate FIA in advance of a DTW-based trafficability assessment and support the prediction of **wet** soils with low strength.

Recent investigations have shown, that machine learning algorithms can successfully be used in the field of digital soil mapping (Baltensweiler et al., 2021) and soil moisture mapping (Ågren et al., 2021). We state, that enhanced computational methods can be deployed for trafficability predictions. An adequate consideration of site effects (Heung et al., 2016), non-linear hydrological processes (Melander et al., 2020) and weather data (Mattila and Tokola, 2019) could facilitate improved predictive accuracy. Moreover, several variables can be fused with basic DTW predictions, including remotely sensed retrievals of soil moisture (e.g. Reichle et al., 2020), as conceived by Schönauer et al. (2021).

An appropriate prediction of soil strength and trafficability would enhance sustainable forest management and in turn cost-efficient and environmentally sound harvesting operations (Murphy et al., 2007; Vega-Nieva et al., 2009; White et al., 2012; Mohtashami et al., 2017; Mattila and Tokola, 2019; Picchio et al., 2020; Uusitalo et al., 2020). The DTW concept entails low demands of input data and is numerically robust, allowing for a calculation using DEMs with different resolutions (ideally lower than 5 m). Although rutting per se is possibly not avoidable by the application of DTW maps (Mohtashami et al., 2017; Schönauer et al., 2021a), the usage could support harvesting operations through better guidance of machine operators through forest sites, as practical use of DTW-maps has been witnessed, for example in Canada and Sweden. By this, sensitive areas can be effectively avoided or reinforced with brush mats and so can the thereby caused deleterious sediment transport in sensitive areas and perennial streams (White et al., 2012; Ågren et al., 2015; Kuglerová et al., 2017; Lidberg et al., 2020).

5. Conclusions

Field trials conducted at various sites across Europe revealed strong temporal variations of SMC, which can be associated with soil strength. During a period of relatively low precipitation, it was possible to

correctly predict a high share of wet soils occurring by DTW maps which represented overall dry conditions, especially on sites in Finland and Poland. The prevailingly sandy soil texture at these sites might contribute to a topography-derived and geometric flow accumulation. On the contrary, on German study sites, only 35% of wet soils matched with the predictions made, considering $DTW_{4.00}$ maps (Fig. 8). As compared to predictions of soil moisture, the prediction of soil strength showed to be less accurate. Although overall accuracy reached 76% when binary values of soil strength were compared to $DTW_{4.00}$ maps, 66% of low values occurred on measuring points possessing a $DTW_{4.00}$ index greater than 1 m. We state, that present site effects, such as soil characteristics led to non-linear water accumulation and peculiar spatial variations of soil moisture and strength. The choice of an individual map-scenario enabled accuracy improvements for given sites. Still, the intended representation of moisture conditions by DTW scenarios could not be proven by the data from the conducted time-series. Therefore, no general rules could be formulated in terms of which FIA would result in best site- and condition-specific DTW performance. Current research already addresses this issue and aims in a clear direction – machine learning. Improved supervised learning algorithms may merge spatial with temporal information, cope with non-linear dynamics of soil state, and support the creation of more accurate trafficability maps in return.

CRediT authorship contribution statement

Marian Schönauer: Conceptualization, Methodology, Formal analysis, Visualization, Investigation, Resources, Writing – original draft, Writing – review & editing. **Kari Väätäinen:** Investigation, Resources, Writing – review & editing. **Robert Prinz:** Investigation, Resources, Writing – review & editing. **Harri Lindeman:** Investigation, Resources. **Dariusz Pszenny:** Investigation, Resources, Writing – review & editing. **Martin Jansen:** Investigation, Resources, Writing – review & editing, Supervision. **Joachim Maack:** Writing – original draft, Writing – review & editing. **Bruce Talbot:** Writing – review & editing. **Rasmus Astrup:** Writing – review & editing, Project administration, Funding acquisition. **Dirk Jaeger:** Conceptualization, Methodology, Writing – review & editing, Supervision, Project administration, Funding acquisition.

Declaration of Competing Interest

The authors declare that they have no known competing financial interests or personal relationships that could have appeared to influence the work reported in this paper.

Acknowledgements

We acknowledge the valuable suggestions of the three anonymous reviewers, who contributed to the improvement of the paper.

Funding

This work was supported by the Bio Based Industries Joint Undertaking under the European Union's Horizon 2020 research and innovation program, TECH4EFFECT Knowledge and Technologies for Effective Wood Procurement—project, [grant number 720757]; by the cooperation project "BefahrGut" funded by the State of North Rhine-Westphalia, Germany, through its Forest Education Center FBZ/State Enterprise Forestry and Timber NRW, Arnsberg/Germany; and by the Eva Mayr-Stihl Stiftung. The APC was funded by the Open Access Publication Funds of the University of Göttingen.

References

Ågren, A., Lidberg, W., Ring, E., 2015. Mapping Temporal Dynamics in a Forest Stream Network—Implications for Riparian Forest Management. Forests 6, 2982–3001. https://doi.org/10.3390/f6092982.

Ågren, A., Lidberg, W., Strömgren, M., Ogilvie, J., Arp, P.A., 2014. Evaluating digital terrain indices for soil wetness mapping – a Swedish case study. Hydrol. Earth Syst. Sci. 18, 3623–3634. https://doi.org/10.5194/hess-18-3623-2014.

Ågren, A.M., Larson, J., Paul, S.S., Laudon, H., Lidberg, W., 2021. Use of multiple LIDAR-derived digital terrain indices and machine learning for high-resolution national-scale soil moisture mapping of the Swedish forest landscape. Geoderma 404, 115280. https://doi.org/10.1016/j.geoderma.2021.115280.

Awaida, A., and Westervelt, J., 2020. USA: Geographic Resources Analysis Support System (GRASS GIS) Software.

Baltensweiler, A., Walthert, L., Hanewinkel, M., Zimmermann, S., Nussbaum, M., 2021. Machine learning based soil maps for a wide range of soil properties for the forested area of Switzerland. Geoderma Regional 27, e00437. https://doi.org/10.1016/j.geodrs.2021.e00437.

Bartels, S.F., Caners, R.T., Ogilvie, J., White, B., Macdonald, S.E., 2018. Relating Bryophyte Assemblages to a Remotely Sensed Depth-to-Water Index in Boreal Forests. Front. Plant Sci. 9 https://doi.org/10.3389/fpls.2018.00858.

Bates, P.C., Blinn, C.R., Alm, A.A., 1993. Harvesting impacts on quaking aspen regeneration in northern Minnesota. Can. J. For. Res. 23 (11), 2403–2412. https://doi.org/10.1139/x93-297.

Beylich, A., Oberholzer, H.-R., Schrader, S., Höper, H., Wilke, B.-M., 2010. Evaluation of soil compaction effects on soil biota and soil biological processes in soils. Soil Tillage Res. 109 (2), 133–143. https://doi.org/10.1016/j.still.2010.05.010.

Bishop, K., Seibert, J., Nyberg, L., Rodhe, A., 2011. Water storage in a till catchment. II: Implications of transmissivity feedback for flow paths and turnover times. Hydrol. Process. 25, 3950–3959. https://doi.org/10.1002/Hyp.8355.

Bivand, R.S., 2021. rgrass7: Interface Between GRASS 7 Geographical Information System and R, https://CRAN.R-project.org/package=rgrass7.

Cambi, M., Certini, G., Neri, F., Marchi, E., 2015. The impact of heavy traffic on forest soils: A review. For. Ecol. Manage. 338, 124–138. https://doi.org/10.1016/j.foreco.2014.11.022.

Campbell, D.M.H., White, B., Arp, P.A., 2013. Modeling and mapping soil resistance to penetration and rutting using LiDAR-derived digital elevation data. J. Soil Water Conserv. 68 (6), 460–473. https://doi.org/10.2489/jswc.68.6.460.

Climate Service Center Germany, 2021. Version 1.2. https://www.gerics.de/imperia/md/content/csc/projekte/klimasignalkarten/gerics_klimaausblick_germany_version1.2_deutsch.pdf. (Accessed 13 November 2021).

Coleman, T.L., Agbu, P.A., Montgomery, O.L., 1993. Spectral differentiation of surface soils and soil properties: Is it possible from space platforms? Soil Sci. 155 (4), 283–293.

Deutscher Wetterdienst, 2019. *Deutscher Klimaatlas*. Accessed July 24, 2019, https://www.dwd.de/DE/klimaumwelt/klimaatlas/klimaatlas_node.html.

Dobos, E., Montanarella, L., Nègre, T., Micheli, E., 2001. A regional scale soil mapping approach using integrated AVHRR and DEM data. Int. J. Appl. Earth Obs. Geoinf. 3 (1), 30–42. https://doi.org/10.1016/S0303-2434(01)85019-4.

Eijkelkamp, 2013. *User Manual for the Moisture Meter type HH2*. Accessed August 07, 2020, https://www.eijkelkamp.com/download.php?file=M1142602e_Soil_moisture_meter_f1ab.pdf.

Fassnacht, F.E., Latifi, H., Stereńczak, K., Modzelewska, A., Lefsky, M., Waser, L.T., Straub, C., Ghosh, A., 2016. Review of studies on tree species classification from remotely sensed data. Remote Sens. Environ. 186, 64–87. https://doi.org/10.1016/j.rse.2016.08.013.

Finnish Meteorological Institute, 2021. *Observation stations*. Accessed May 05, 2021, https://en.ilmatieteenlaitos.fi/observation-stations?filterKey=groups&filterQuery=precipitation.

Fox, J., Weisberg, S., 2019. An R Companion to Applied Regression. Sage, Thousand Oaks CA.

Heung, B., Ho, H.C., Zhang, J., Knudby, A., Bulmer, C.E., Schmidt, M.G., 2016. An overview and comparison of machine-learning techniques for classification purposes in digital soil mapping. Geoderma 265, 62–77. https://doi.org/10.1016/j.geoderma.2015.11.014.

Horn, R., Vossbrink, J., Peth, S., Becker, S., 2007. Impact of modern forest vehicles on soil physical properties. For. Ecol. Manage. 248 (1-2), 56–63. https://doi.org/10.1016/j.foreco.2007.02.037.

Hu, Z., Islam, S., Cheng, Y., 1997. Statistical characterization of remotely sensed soil moisture images. Remote Sens. Environ. 61 (2), 310–318. https://doi.org/10.1016/S0034-4257(97)89498-9.

IMGW-PIB, 2021. *Observation stations*. Accessed May 05, 2021, https://www.imgw.pl/en/institute/imgw-pib.

Jones, M.-F., Arp, P., 2019. Soil Trafficability Forecasting. OJF 9, 296–322. https://doi.org/10.4236/ojf.2019.94017.

Jones, M.-F., Arp, P.A., 2017. Relating Cone Penetration and Rutting Resistance to Variations in Forest Soil Properties and Daily Moisture Fluctuations. Open Journal of Soil Science 07 (07), 149–171. https://doi.org/10.4236/ojss.2017.77012.

Kuglerová, L., Hasselquist, E.M., Richardson, J.S., Sponseller, R.A., Kreutzweiser, D.P., Laudon, H., 2017. Management perspectives on Aqua incognita : Connectivity and cumulative effects of small natural and artificial streams in boreal forests. Hydrol. Process. 31 (23), 4238–4244. https://doi.org/10.1002/hyp.v31.2310.1002/hyp.11281.

Kuhn, M., 2020. caret: Classification and Regression Training. Accessed November 13, 2021, https://CRAN.R-project.org/package=caret.

Kurczyński, Z., Bakuła, K., 2013. The selection of aerial laser scanning parameters for countrywide digital elevation model creation. In: *13th SGEM GeoConference on Informatics, Geoinformatics and Remote Sensing. SGEM2013 Conference Proceedings*, pp. 695–702.

Labelle, E.R., Jaeger, D., 2019. Effects of steel flexible tracks on forwarder peak load distribution: Results from a prototype load test platform. Croatian J. Forest Eng. 40, 1–23.

Leach, J.A., Lidberg, W., Kuglerová, L., Peralta-Tapia, A., Ågren, A., Laudon, H., 2017. Evaluating topography-based predictions of shallow lateral groundwater discharge zones for a boreal lake-stream system. Water Resour. Res. 53 (7), 5420–5437. https://doi.org/10.1002/2016WR019804.

Lenth, R.V., Buerkner, P., Herve, M., Love, J., Riebl, H., Singmann, H., 2019. emmeans: Estimated Marginal Means aka Least-Squares Means, Accessed November 13, 2021. https://CRAN.R-project.org/package=emmeans.

Lidberg, W., Nilsson, M., Ågren, A., 2020. Using machine learning to generate high-resolution wet area maps for planning forest management: A study in a boreal forest landscape. Ambio 49 (2), 475–486. https://doi.org/10.1007/s13280-019-01196-9.

Matthews, B.W., 1975. Comparison of the predicted and observed secondary structure of T4 phage lysozyme. Biochimica et Biophysica Acta (BBA) - Protein Structure 405 (2), 442–451. https://doi.org/10.1016/0005-2795(75)90109-9.

Mattila, U., Tokola, T., 2019. Terrain mobility estimation using TWI and airborne gamma-ray data. J. Environ. Manage. 232, 531–536. https://doi.org/10.1016/j.jenvman.2018.11.081.

McNabb, D.H., Startsev, A.D., Nguyen, H., 2001. Soil Wetness and Traffic Level Effects on Bulk Density and Air-Filled Porosity of Compacted Boreal Forest Soils. Soil Sci. Soc. Am. J. 65 (4), 1238–1247. https://doi.org/10.2136/sssaj2001.6541238x.

Melander, L., Einola, K., Ritala, R., 2020. Fusion of open forest data and machine fieldbus data for performance analysis of forest machines. Eur. J. Forest Res. 139 (2), 213–227. https://doi.org/10.1007/s10342-019-01237-8.

Mohtashami, S., Eliasson, L., Jansson, G., Sonesson, J., 2017. Influence of soil type, cartographic depth-to-water, road reinforcement and traffic intensity on rut formation in logging operations: a survey study in Sweden. Silva Fennica 51. https://doi.org/10.14214/sf.2018.

Murphy, P.N.C., Ogilvie, J., Arp, P., 2009. Topographic modelling of soil moisture conditions: A comparison and verification of two models. Eur. J. Soil Sci. 60, 94–109. https://doi.org/10.1111/j.1365-2389.2008.01094.x.

Murphy, P.N.C., Ogilvie, J., Connor, K., Arp, P.A., 2007. Mapping wetlands: A comparison of two different approaches for New Brunswick, Canada. Wetlands 27, 846–854. https://doi.org/10.1672/0277-5212(2007)27[846:MWACOT]2.0.CO;2.

Murphy, P.N.C., Ogilvie, J., Meng, F.-R., White, B., Bhatti, J.S., Arp, P.A., 2011. Modelling and mapping topographic variations in forest soils at high resolution: A case study. Ecol. Model. 222 (14), 2314–2332. https://doi.org/10.1016/j.ecolmodel.2011.01.003.

Niemi, M.T., Vastaranta, M., Vauhkonen, J., Melkas, T., Holopainen, M., 2017. Airborne LiDAR-derived elevation data in terrain trafficability mapping. Scand. J. For. Res. 32 (8), 762–773. https://doi.org/10.1080/02827581.2017.1296181.

O'Callaghan, J.F., Mark, D.M., 1984. The extraction of drainage networks from digital elevation data. Computer vision, graphics, and image processing 28 (3), 323–344.

Oltean, G.S., Comeau, P.G., White, B., 2016. Linking the Depth-to-Water Topographic Index to Soil Moisture on Boreal Forest Sites in Alberta. Forest Science 62 (2), 154–165. https://doi.org/10.5849/forsci.15-054.

Picchio, R., Latterini, F., Mederski, P.S., Tocci, D., Venanzi, R., Stefanoni, W., Pari, L., 2020. Applications of GIS-Based Software to Improve the Sustainability of a Forwarding Operation in Central Italy. Sustainability 12 (14), 5716. https://doi.org/10.3390/su12145716.

Poltorak, B.J., Labelle, E.R., Jaeger, D., 2018. Soil displacement during ground-based mechanized forest operations using mixed-wood brush mats. Soil Tillage Res. 179, 96–104. https://doi.org/10.1016/j.still.2018.02.005.

Powers, D.M.W., 2011. Evaluation: from precision, recall and F-measure to ROC, informedness, markedness and correlation. International Journal of Machine Learning Technology 2, 1.

QGIS.org., 2020. *QGIS Geographic Information System*. Open Source Geospatial Foundation Project.

R Core Team, 2020. R: A Language and Environment for Statistical Computing. The R Foundation for Statistical Computing, Vienna, Austria.

Rab, M.A., 2004. Recovery of soil physical properties from compaction and soil profile disturbance caused by logging of native forest in Victorian Central Highlands, Australia. For. Ecol. Manage. 191 (1-3), 329–340. https://doi.org/10.1016/j.foreco.2003.12.010.

Reichle, R., Lannoy, G. de, Koster, R., Crow, W., Kimball, J., and Liu, Q., 2020. *SMAP L4 Global 3-hourly 9 km EASE-Grid Surface and Root Zone Soil Moisture Geophysical Data, Version 5*. NASA National Snow and Ice Data Center DAAC.

Salmivaara, A., Launiainen, S., Perttunen, J., Nevalainen, P., Pohjankukka, J., Ala-Ilomäki, J., Sirén, M., Laurén, A., Tuominen, S., Uusitalo, J., Pahikkala, T., Heikkonen, J., Finér, L., 2020. Towards dynamic forest trafficability prediction using open spatial data, hydrological modelling and sensor technology. Forestry 93 (5), 662–674. https://doi.org/10.1093/forestry/cpaa010.

Schönauer, M., 2020. Supplementary data for: Comparison of selected terramechanical test procedures and cartographic indices to predict rutting caused by machine traffic during a cut-to-length thinning-operation. Göttingen Research Online / Data.

Schönauer, M., Hoffmann, S., Maack, J., Jansen, M., Jaeger, D., 2021a. Comparison of Selected Terramechanical Test Procedures and Cartographic Indices to Predict Rutting Caused by Machine Traffic during a Cut-to-Length Thinning-Operation. Forests 12, 113. https://doi.org/10.3390/f12020113.

Seki, K., 2007. *SWRC fit – a nonlinear fitting program with a water retention curve for soils having unimodal and bimodal pore structure*.

Schönauer, M., Maack, J., 2021. R-code for calculating depth-to-water (DTW) maps using GRASS GIS (Version v1). Zenodo. https://doi.org/10.5281/zenodo.5638518.

Schönauer, M., Prinz, R., Väätäinen, K., Astrup, R., Pszenny, D., Lindeman, H., Jaeger, D., 2021. Spatio-temporal prediction of soil moisture using soil maps, topographic indices and NASA Earthdata. Zenodo. https://doi.org/10.5281/zenodo.5691527.

Singh, V.K., Kumar, D., Kashyap, P.S., Singh, P.K., Kumar, A., Singh, S.K., 2020. Modelling of soil permeability using different data driven algorithms based on physical properties of soil. J. Hydrol. 580, 124223. https://doi.org/10.1016/j.jhydrol.2019.124223.

Sohrabi, H., Jourgholami, M., Jafari, M., Tavankar, F., Venanzi, R., Picchio, R., 2021. Earthworms as an Ecological Indicator of Soil Recovery after Mechanized Logging Operations in Mixed Beech Forests. Forests 12, 18. https://doi.org/10.3390/f12010018.

Suvinen, A., Tokola, T., Saarilahti, M., 2009. Terrain trafficability prediction with GIS analysis. Forest Science 55, 433–442. https://doi.org/10.1093/forestscience/55.5.433.

Tarboton, D.G., 1997. A new method for the determination of flow directions and upslope areas in grid digital elevation models. Water Resour. Res. 33 (2), 309–319. https://doi.org/10.1029/96WR03137.

Ustin, S.L., Gamon, J.A., 2010. Remote sensing of plant functional types. New Phytol. 186 (4), 795–816. https://doi.org/10.1111/nph.2010.186.issue-410.1111/j.1469-8137.2010.03284.x.

Uusitalo, J., Ala-Ilomäki, J., Lindeman, H., Toivio, J., Siren, M., 2020. Predicting rut depth induced by an 8-wheeled forwarder in fine-grained boreal forest soils. Annals of forest science 77 (2). https://doi.org/10.1007/s13595-020-00948-y.

Väätäinen, K., Uusitalo, J., Launiainen, S., Peuhkurinen, J., Berqkvist, I., Ala-Ilomäki, J., et al., 2019. *EFFORTE. Validation of developed tools for operational planning*.

Vega-Nieva, D.J., Murphy, P.N.C., Castonguay, M., Ogilvie, J., Arp, P.A., 2009. A modular terrain model for daily variations in machine-specific forest soil trafficability. Can. J. Soil Sci. 89 (1), 93–109. https://doi.org/10.4141/CJSS06033.

Wheeler, B., Torchiano, M., and Torchiano, M.M., 2016. Package 'lmPerm'. *R package version* 2.

White, B., Ogilvie, J., Campbell, D.M.H.M.H., Hiltz, D., Gauthier, B., Chisholm, H.K.H., Wen, H.K., Murphy, P.N.C.N.C., Arp, P.A.A., 2012. Using the Cartographic Depth-to-Water Index to Locate Small Streams and Associated Wet Areas across Landscapes. Canadian Water Resources Journal 37 (4), 333–347. https://doi.org/10.4296/cwrj2011-909.

Zanella, A., Jabiol, B., Ponge, J.F., Sartori, G., De Waal, R., Van Delft, B., Graefe, U., Cools, N., Katzensteiner, K., Hager, H., Englisch, M., 2011. A European morpho-functional classification of humus forms. Geoderma 164 (3-4), 138–145. https://doi.org/10.1016/j.geoderma.2011.05.016.